Appl. Math. and Comp. Sci., 1995, vol.5, No.1, 89–103

THROUGHFLOW OF A BINGHAM FLUID IN A SLOT BETWEEN ROTATING SURFACES OF REVOLUTION

EDWARD WALICKI*, ANNA WALICKA*

This paper contains formulae which define such parameters of the steady laminar flow of a Bingham fluid between rotating surfaces of revolution as the velocity components v_x, v_θ, v_y and pressure p. The linearized equations of motion of the Bingham fluid flow for axial symmetry in the intrinisic curvilinear coordinate system x, θ, y are used. The solutions of the equations of motion have been illustrated by the example of fluid flow through the slot of constant thickness between rotating disks and between rotating spherical surfaces.

1. Introduction

The steady laminar flows of incompressible or compressible viscous Newtonian fluid in a narrow space between rotating surfaces of revolution have been examined theoretically and experimentally. Analytical studies of these flows have been presented in (McAlister and Rice, 1970; Walicka, 1989).

The problem of viscous Newtonian throughflow between rotating surfaces of revolution, the shapes of which are described by the functions satisfying any conditions for which similar solutions exist, is solved by McAlister and Rice (1970). The same flow in a more general statement is examined in (Walicka, 1989).

Many fluids of engineering interest appear to exhibit yield behaviour, where flow occurs only when the imposed stress exceeds a critical yield stress. Such viscoplastic fluids, which were first analyzed systematically by Prager (1961), Coleman *et al.* (1966) and Schulman (1975, 1982) include some polymer liquid crystals and some filled thermoplastics.

To describe the rheological behaviour of viscoplastic (non-Newtonian) fluids in complex geometries the Bingham model is often used (cf. e.g. Dai and Bird, 1981; Lipscomb and Dean, 1984; Sandru and Camenschi, 1988; Walicka and Walicki, 1994).

Our interest in this paper is to examine the steady laminar flow of a Bingham fluid in the slot of small thickness between rotating curvilinear surfaces of revolution having a common axis of symmetry as shown in Fig. 1. The problem is solved with the partial influence of inertia terms in equations of motion (rotational inertia), i.e., under the assumption that the velocity of circumferential flow is great in comparison to the velocity of longitudinal flow.

* Technical University of Zielona Góra, Faculty of Mechanics, ul. Podgórna 50, 65–246 Zielona Góra, Poland

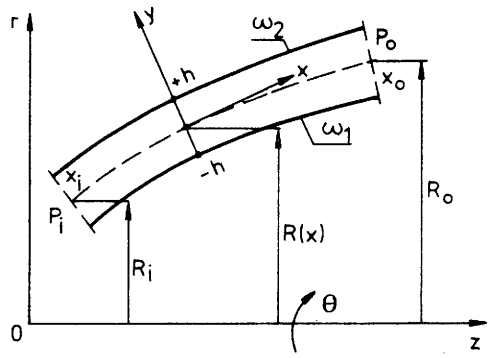

Fig. 1. Slot of small thickness between rotating surfaces of revolution. Coordinate system and geometry of surfaces.

2. Equations of Motion in a Thin Layer

The configuration of the flow is shown in Fig. 1. The curvilinear surfaces are discribed by function $R(x)$ which denotes the radius of the median surface between the rotating surfaces plus function $h(x)$ which denotes the distance to each surface from the median. An intrinsic curvilinear orthogonal coordinate system x, θ, y is depicted in Fig. 1. The inner surface has angular velocity ω_1 and the outer surface has angular velocity ω_2.

The physical parameters of the flow are the velocity components v_x, v_θ, v_y and pressure p. With regard to axial symmetry of the flow these parameters are not dependent on the angle θ.

Let us make the assumption typical for the flow in a narrow space that

$$h(x) \ll R(x)$$

and the assumption on the velocity orders which can be expressed in the form

$$v_x = 0\left(v_m \frac{h_m}{R_m}\right), \qquad v_\theta = 0(v_m), \qquad v_y = 0\left(v_m \frac{h_m^2}{R_m^2}\right)$$

where v_m is the mean value of the velocity of circumferential flow and h_m, R_m are, respectively, the mean values of $h(x)$ and $R(x)$ in the slot.

Taking into consideration the above assumptions we can make order — of — magnitude arguments in the equations governing the steady flow of a Bingham fluid.

If the asymptotic transformations have been made, the same as in (Walicka, 1989), these equations can be reduced to a simpler form

$$\frac{1}{R}\frac{\partial(Rv_x)}{\partial x} + \frac{\partial v_y}{\partial y} = 0 \tag{1}$$

$$-\rho v_\theta^2 \frac{R'}{R} = -\frac{\partial p}{\partial x} + \frac{\partial}{\partial y}\left(L\frac{\partial v_x}{\partial y}\right) \tag{2}$$

$$0 = \frac{\partial}{\partial y}\left(L\frac{\partial v_\theta}{\partial y}\right) \tag{3}$$

$$0 = \frac{\partial}{\partial y} \tag{4}$$

where

$$L = \left[\tau_0 + \left(\mu\left|\frac{\partial v_\theta}{\partial y}\right|\right)\right]\left|\frac{\partial v_\theta}{\partial y}\right|^{-1} \tag{5}$$

is the function of viscosity. The "prime" denotes everywhere derivation with respect to x.

After asymptotic transformations the equation of motion in the y-direction indicates that

$$p(x, y) = p(x) \tag{6}$$

The problem statement is complete after specification of boundary conditions. These conditions for the velocity components are stated as follows

$$v_x(x \pm h) = 0 \tag{7}$$

$$v_\theta(x, -h) = R\omega_1, \qquad v_\theta(x, +h) = R\omega_2 \tag{8}$$

$$v_y(x, \pm h) = 0 \tag{9}$$

The boundary conditions for the pressure are

$$p(x_i) = p_i, \qquad p(x_0) = p_0 \tag{10}$$

thus, x_i denotes the inlet coordinate and x_0 – the outlet coordinate.

3. Solution of the Equations of Motion

Integrating in sequence equations (2)–(4) with respect to y in the interval $-h \leq y \leq +h$ and determining the arbitrary constants from the boundary conditions (7) and (8) we obtain

$$v_\theta = \frac{R}{2}\left[\omega_2 + \omega_1 + (\omega_2 - \omega_1)\frac{y}{h}\right] \tag{11}$$

$$\begin{aligned} v_x = {} & \frac{y^2 - h^2}{2L}\frac{\mathrm{d}p}{\mathrm{d}x} - \frac{\rho R R'}{4L}\left[\frac{y^2 - h^2}{2}(\omega_2 + \omega_1)^2\right. \\ & \left. + \frac{y^3 - yh^2}{3h}(\omega_2^2 + \omega_1^2) + \frac{y^4 - h^4}{12h^2}(\omega_2 + \omega_1)^2\right] \end{aligned} \tag{12}$$

with

$$L = \frac{2H}{R|\omega_2 - \omega_1|}\left(\tau_0 + \frac{\mu R(\omega_2 - \omega_1)}{2h}\right) \tag{13}$$

Next integrating the equation of continuity (1) across the slot and taking into account boundary conditions (7) and (9) we have

$$\int_{-h}^{+h} v_x \, \mathrm{d}y = \frac{C^*}{R(x)} \tag{14}$$

where C^* is an arbitrary constant. Substituting (12) into (14) we find

$$\frac{\mathrm{d}p}{\mathrm{d}x} = \frac{CL}{Rh^3} + \frac{\rho R R'}{4}\Omega^2 \tag{15}$$

where

$$\Omega^2 = (\omega_2 - \omega_1)^2 + \frac{1}{5}(\omega_2 - \omega_1)^2 \tag{16}$$

and C is a new arbitrary constant.

Integrating (15) and taking into account boundary conditions (10) we obtain

$$p(x) = B(x) + \frac{[A(x) - A_0](p_i - B_i) - [A(x) - A_i](p_0 - B_0)}{A_i - A_0} \tag{17}$$

the constant C is equal to

$$C = \frac{p_i - p_0 - (B_i - B_0)}{A_i - A_0} \tag{18}$$

where:

$$\begin{aligned} A(x) &= \int \frac{L}{Rh^3}\,\mathrm{d}x, \quad A_i = A(x_i), \quad A_0 = A(x_0) \\ B(x) &= \frac{\rho R^2 \Omega^2}{8}, \qquad B_i = B(x_i), \quad B_0 = B(x_0) \end{aligned} \tag{19}$$

Substituting (15) into (12) we may present the formula for velocity component v_x in the form

$$\begin{aligned} v_x = -\frac{C}{2Rh}\left(1 - \frac{y^2}{h^2}\right) - \frac{\rho R R' h^2}{240L}\Bigg[\left(1 - 6\frac{y^2}{h^2} + 5\frac{y^4}{h^4}\right)(\omega_2 - \omega_1)^2 \\ -20\frac{y}{h}\left(1 - \frac{y^2}{h^2}\right)(\omega_2^2 - \omega_1^2)\Bigg] \end{aligned} \tag{20}$$

Taking into account the result obtained above in (1) and integrating this equation with respect to y we get the formula for velocity component v_y

$$\begin{aligned} v_y = \frac{1}{R}\frac{\partial}{\partial x}\Bigg\{\frac{C}{6}\frac{y}{h}\left(3 - \frac{y^2}{h^2}\right) + \frac{\rho R^2 R' h^3}{240L}\Bigg[\frac{y}{h}\left(1 - 2\frac{y^2}{h^2} + \frac{y^4}{h^4}\right) \\ \times (\omega_2 - \omega_1)^2 + 5\left(1 - 2\frac{y^2}{h^2} + \frac{y^4}{h^4}\right)(\omega_2^2 - \omega_1^2)\Bigg]\Bigg\} \end{aligned} \tag{21}$$

Note that for Newtonian fluid we have: $L = \mu_{\text{Newt.}}$, i.e., the function of viscosity passes on Newtonian shear (dynamic) viscosity. In this case, all the above formulae are identical with those given for Newtonian flow and they are true for all the values of ω_1 and ω_2.

The solution for Bingham fluid presented here is also true for all the values of ω_1 and ω_2, except when $\omega_1 = \omega_2$, because in this case formula (13) for the function of viscosity is no longer valid.

4. Examples

4.1. Non-dimensional Form of the Solution for the Slot of Constant Thickness

Equations (11), (13) and (16)–(20) can be made non-dimensional by using the following parameters

$$\begin{aligned}
&\widetilde{x} = \frac{x}{R_0}, \qquad \widetilde{R_0} = \frac{R}{R_0}, \qquad \varepsilon = \frac{R_i}{R_0}, \qquad \widetilde{y} = \frac{y}{h} \\
&\widetilde{v}_x = -\frac{2R_0 h}{C} v_x, \qquad \widetilde{v}_\theta = \frac{v_\theta}{R_0 \omega_1}, \qquad \widetilde{p} = \frac{p}{p_0} \\
&\widetilde{L}(\widetilde{x}) = \frac{L(x)}{\mu}, \qquad \widetilde{A}(\widetilde{x}) = \frac{h^3}{\mu} A(x), \qquad \delta = \frac{p_i}{p_0} \\
&f = \frac{\omega_2}{\omega_1}, \qquad F = \frac{\Omega^2}{\omega_1^2}, \qquad G = \frac{G_0}{|f-1|}, \qquad G_0 = \frac{2h\tau_0}{\mu R_0 \omega_1}
\end{aligned} \tag{22}$$

hence, we have

$$\widetilde{p} = \widetilde{B}(\widetilde{x}) + \frac{\delta - 1 + \widetilde{B}_0 - \widetilde{B}_i}{\widetilde{A}_i - \widetilde{A}_0} \widetilde{A}(\widetilde{x}) + \frac{\widetilde{A}_i(1 - \widetilde{B}_0) - \widetilde{A}_0(\delta - \widetilde{B}_i)}{\widetilde{A}_i - \widetilde{A}_0} \tag{23}$$

$$\widetilde{v}_x = \frac{1}{\widetilde{R}}(1 - \widetilde{y}^2) + \widetilde{\Pi}_c \widetilde{\Pi}(\widetilde{R}) \widetilde{R} \widetilde{R}' V_x(\widetilde{y}) \tag{24}$$

$$\widetilde{v}_\theta = \widetilde{R} V_\theta(\widetilde{y}) \tag{25}$$

where

$$\begin{aligned}
&V_x(\widetilde{y}) = (1 - 6\widetilde{y}^2 + 5\widetilde{y}^4)(f-1)^2 - 20(\widetilde{y} - \widetilde{y}^3)(f^2 - 1) \\
&V_\theta(\widetilde{y}) = \frac{1}{2}\Big[f + 1 + \widetilde{y}(f-1)\Big], \qquad \widetilde{A}(\widetilde{x}) = \int \left(\frac{G}{\widetilde{R}^2} + \frac{1}{\widetilde{R}}\right) \mathrm{d}\widetilde{x} \\
&\widetilde{A}_i = \widetilde{A}(\widetilde{x}_i), \qquad \widetilde{A}_0 = \widetilde{A}(\widetilde{x}_0) \\
&\widetilde{B}(\widetilde{x}) = F P_c \widetilde{R}^2, \qquad \widetilde{B}_i = F P_c \varepsilon^2, \qquad \widetilde{B}_0 = F P_c
\end{aligned} \tag{26}$$

$$\widetilde{\Pi}_c = \frac{P_c(\widetilde{A}_i - \widetilde{A}_0)}{15(\delta - 1 + \widetilde{B}_0 - \widetilde{B}_i)}, \qquad \widetilde{\Pi}(\widetilde{R}) = \frac{\widetilde{R}}{G + \widetilde{R}}$$

Here

$$P_c = \frac{\rho R_0^2 \omega_1^2}{8P_0} = \frac{1}{8Eu} \tag{27}$$

and Eu denotes the Euler number for the circumferential flow in the outlet cross – section of the slot, P_c represents the inertia effects due to the circumferential motion of fluid in the slot.

4.2. Throughflow Between the Parallel Disks

For the parallel disks shown in Fig. 2 the geometric relations are: $R = x$, $R_i = x_i$, $R_0 = x_0$, $\varepsilon = x_i/x_0$. The non-dimensional quantities are: $\widetilde{R} = \widetilde{x}$, $\widetilde{R}_0 = 1$, $\widetilde{R}_i = \varepsilon$, $\widetilde{R}' = 1$, and the non-dimentional formulation assumes the form:

$$\widetilde{p} = FP_c\widetilde{x} + \frac{\delta - 1 + (1-\varepsilon^2)FP_c}{\ln\varepsilon - \left(\frac{1}{\varepsilon} - 1\right)G}\left(\ln\widetilde{x} - \frac{G}{\widetilde{x}}\right) + \frac{\left(\ln\varepsilon - \frac{G}{\varepsilon}\right)(1 - P_c) + G(\delta - FP_c\varepsilon^2)}{\ln\varepsilon - \left(\frac{1}{\varepsilon} - 1\right)G} \tag{28}$$

$$\widetilde{v}_x = \frac{1}{\widetilde{x}}(1 - \widetilde{y}^2) + \widetilde{\Pi}_c \frac{\widetilde{x}^2}{G + \widetilde{x}} V_x(\widetilde{y}) \tag{29}$$

$$\widetilde{v}_\theta = \widetilde{x} V_\theta(\widetilde{y}) \tag{30}$$

where

$$\widetilde{\Pi}_c = \frac{\ln\varepsilon - \left(\frac{1}{\varepsilon} - 1\right)G}{15\left[\delta - 1 + (1-\varepsilon^2)FP_c\right]} P_c \tag{31}$$

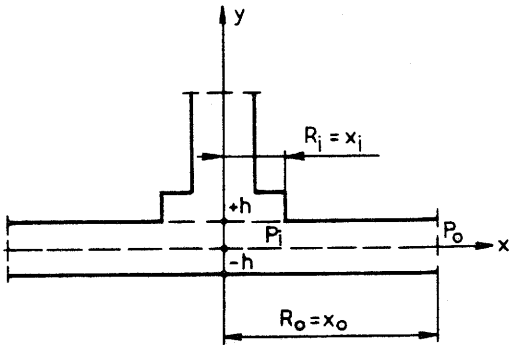

Fig. 2. Slot between parallel disks.

Figures 3 and 4 show the pressure distributions for $f = 0$ (only one disk rotates in the flow configuration presented in Fig. 2) and for two values of the coefficient P_c, namely: $P_c = 2$ and $P_c = 3$. It can be seen from Fig. 4 that the value of $P_c = 3$ and the value of the plasticity coefficient $G_0 = 5$ are the limit values when the cavitation does not occur yet in the flow.

Figures 5 and 6 show the pressure distributions for $f = -1$ (both disks rotate at the same angular velocities, equal, but opposed with respect to the sign) and for two values of the coefficient P_c: $P_c = 2$ and $P_c = 4$. It can be seen from Figs. 3–6 that the pressure decreases with respect to the Newtonian pressure distribution with the increase of the values or coefficients P_c and G_0 and this phenomenon is more intensive for $f = 0$ than for $f = -1$.

Figures 7 and 8 show the profiles of the velocity component $\widetilde{v}_x$ for $f = 0$ and for two values of P_c, namely: for $P_c = 2$ and for $P_c = 3$, respectively. The continuous lines represent the case of Newtonian flow; the dashed lines represent the Bingham fluid flow for $G_0 = 1$, but the dash-dot lines – the flow for $G_0 = 5$. The velocity profiles are made for three positions of the cross-section, for $\widetilde{x} = 0.3$, 0.6 or 0.9, respectively.

It can be seen from these figures that the influence of inertia effects is considerable and it is visible in the cross-sections lying near the outlet to the slot ($\widetilde{x} = 0.9$). The maximum of velocity profiles shifts in the direction of the rotating disk with the increase of P_c. In the middle regions of the slot the inertia effects are inconsiderable (i.e., the differences between the velocity curves are very small for $\widetilde{x} = 0.6$ and for all the values of P_c and G_0).

Figure 9 shows the "halves" of graphs of the velocity profiles $\widetilde{v}_x$ for $f = -1$ and for two values of P_c, namely: $P_c = 2$ (upper graphs) and $P_c = 4$ (lower graphs); the continuous lines represent the case of Newtonian flow, the dashed lines – the case of the Bingham flow for $G_0 = 1$, but the dash-dot lines – the same flow for $G_0 = 5$.

In this case, the velocity curves are symmetrical with respect to the median surface of the slot and the inertia effects have also the same nature as that in the previous case where $f = 0$. It is easy to see from eqn. (25) that the profiles of velocity component $\widetilde{v}_\theta$ are always straight lines.

4.3. Throughflow Between the Concentric Spherical Surfaces

For the concentric spherical surfaces shown in Fig. 10 the geometric relations are given as follows:

$$R = R_s \sin\varphi, \qquad R_i = R_s \sin\varphi_i, \qquad R_0 = R_s \sin\varphi_0$$

$$\varphi = \frac{x}{R_s}, \qquad \varepsilon = \frac{\sin\varphi_i}{\sin\varphi_0}$$

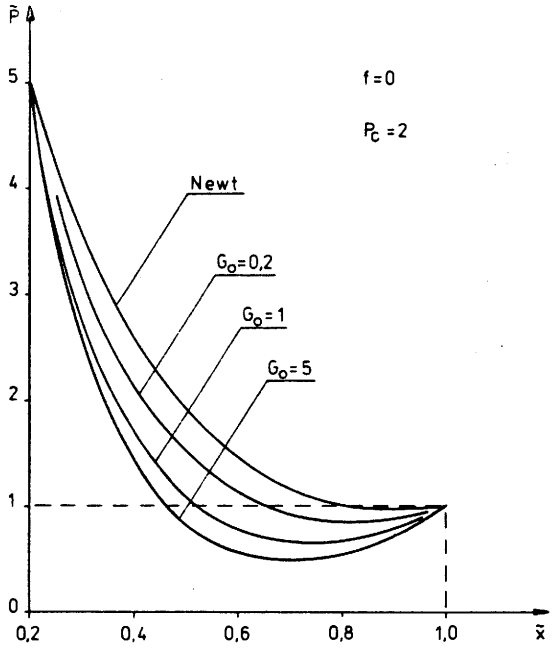

Fig. 3. Dimensionless pressure distributions for the flow between parallel disks for the value of $P_c = 2$ and $f = 0$ (only one disk rotates) vs. G_0 as a parameter.

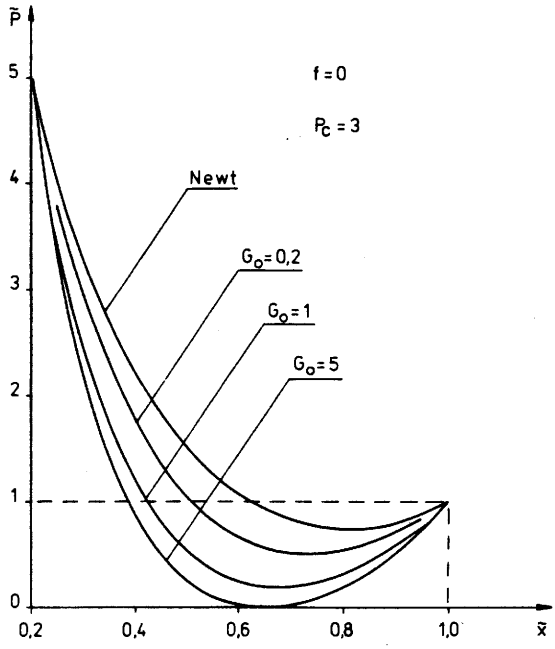

Fig. 4. Dimensionless pressure distributions for the flow between parallel disks for the value of $P_c = 3$ and $f = 0$.

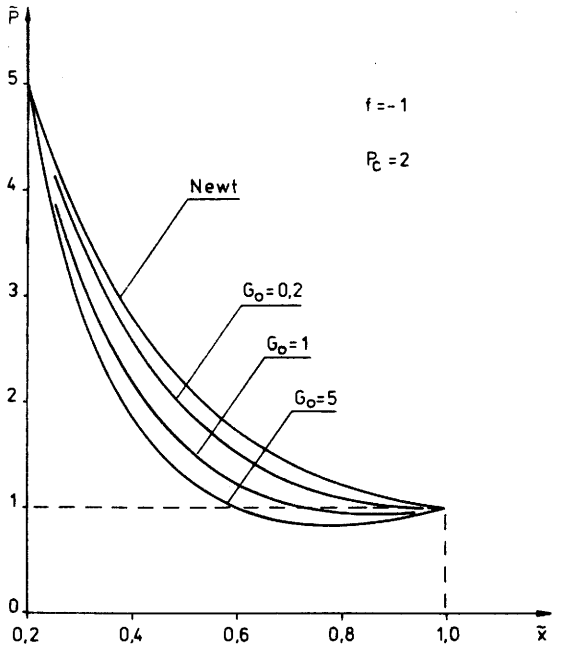

Fig. 5. Dimensionless pressure distributions for the flow between parallel disks for the values: $P_c = 2$ and $f = -1$ (both disks rotate at the same angular velocities, equal, but opposed with respect to the sign).

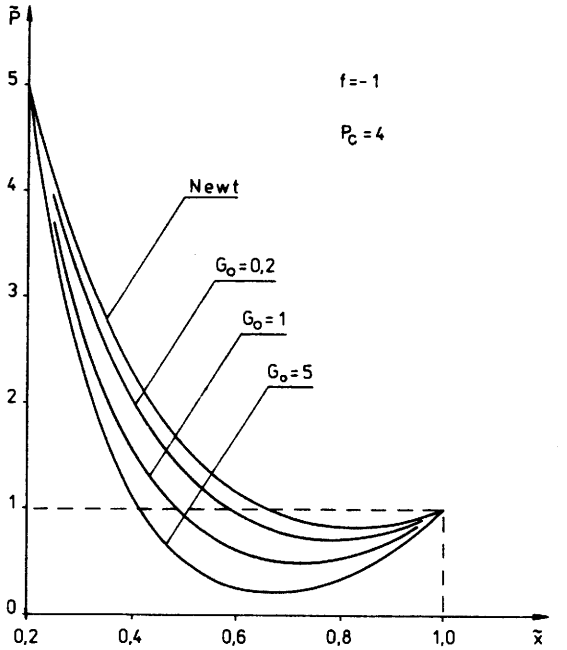

Fig. 6. Dimensionless pressure distributions for the flow between parallel disks for the values: $P_c = 4$ and $f = -1$.

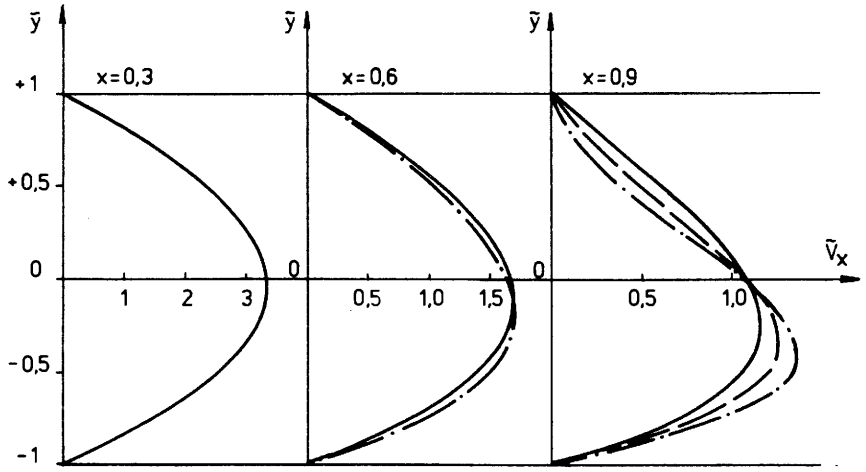

Fig. 7. Dimensionless profiles of the velocity component $\tilde{v}_x$ for the flow between parallel disks for $f = 0$ and $P_c = 2$ at the cross-section described by $\tilde{x} = 0.3$, $\tilde{x} = 0.6$ and $\tilde{x} = 0.9$.

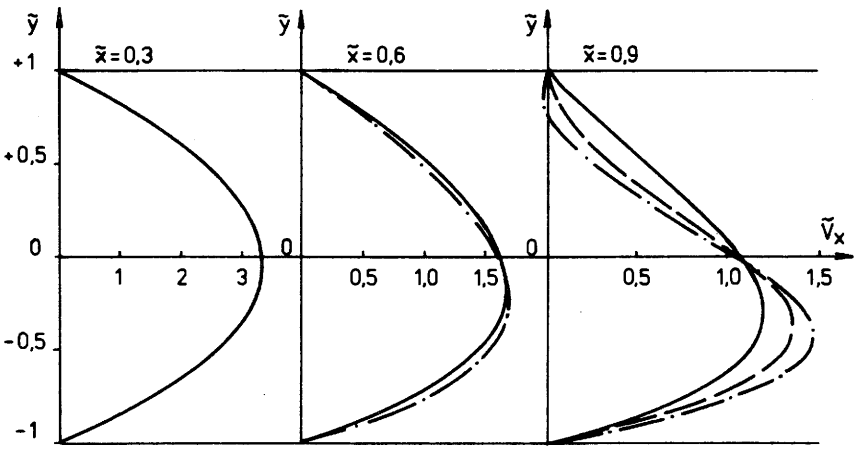

Fig. 8. Dimensionless profiles of the velocity component $\tilde{v}_x$ for the flow between parallel disks for the values: $f = 0$ and $P_c = 3$.

The non-dimensional quantities are (for $\varphi_0 = 90°$): $\tilde{R} = \sin\varphi$, $\tilde{R}_0 = 1$, $\tilde{R}_i = \varepsilon = \sin\varphi_i$, $\tilde{x} = \varphi$, and the non-dimensional formulation assumes the form:

$$\tilde{p} = FP_c \sin^2\varphi + \frac{\delta - 1 + (1 - \sin^2\varphi_i)FP_c}{\ln \operatorname{tg}\frac{\varphi_i}{2} - G \operatorname{ctg}\varphi_i}\left(\ln \operatorname{tg}\frac{\varphi}{2} - G \operatorname{ctg}\varphi\right) + 1 - FP_c \tag{32}$$

$$\tilde{v}_x = \frac{1}{\sin\varphi}(1 - \tilde{y}^2) + \tilde{\Pi}_c \frac{\sin^2\varphi}{G + \sin\varphi} V_x(\tilde{y}) \tag{33}$$

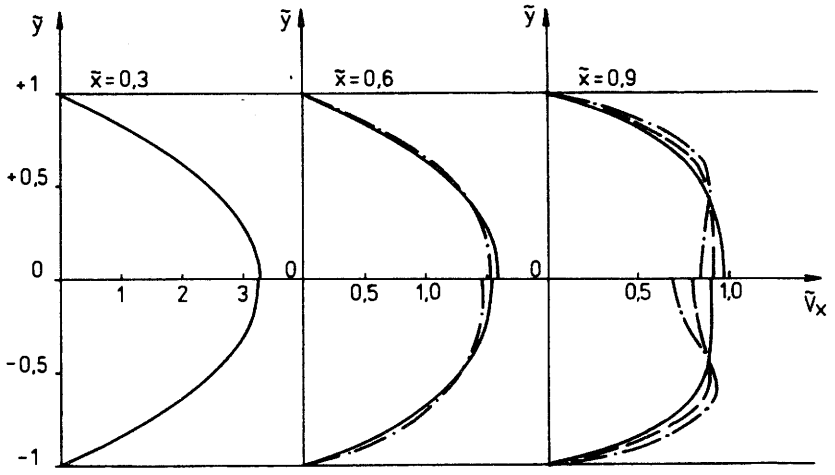

Fig. 9. Dimensionless profiles of the velocity component $\tilde{v}_x$ for the flow between parallel disks for the value of $f = -1$; the upper graphs are made for $P_c = 2$, the lower ones – for $P_c = 4$.

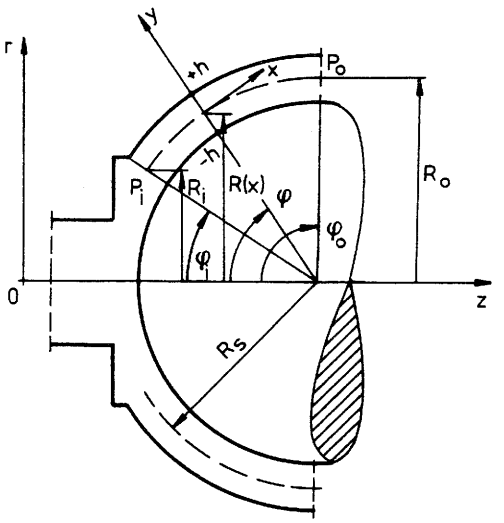

Fig. 10. Slot between concentric spherical surfaces.

$$\tilde{v}_\theta = \sin\varphi V_\theta(\tilde{y}) \tag{34}$$

where

$$\tilde{\Pi}_c = \frac{\ln \operatorname{tg}\frac{\varphi_i}{2} - G\operatorname{ctg}\varphi_i}{15\left[\delta - 1 + (1-\sin^2\varphi_i)FP_c\right]} P_c \tag{35}$$

Figures 11–14 show the pressure distributions for $f = 0$ and for $f = -1$, respectively, for two values of P_c, namely: $P_c = 2$ or $P_c = 4$, and for different values of G_0.

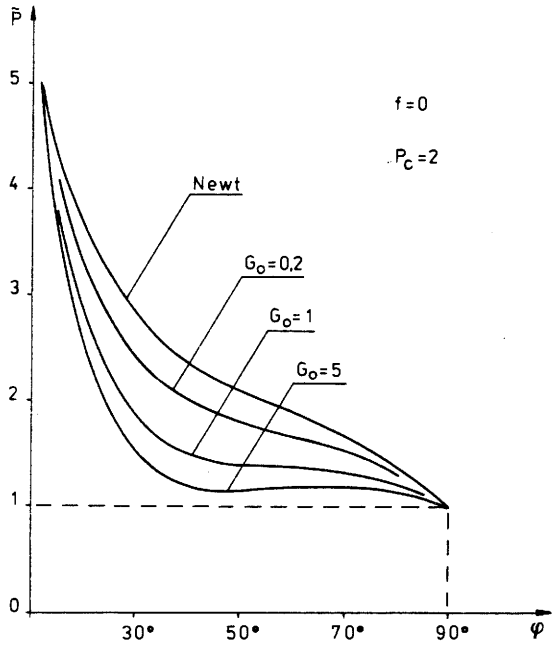

Fig. 11. Dimensionless pressure disributions for the flow between concentric spherical surfaces for $f = 0$ and $P_c = 2$.

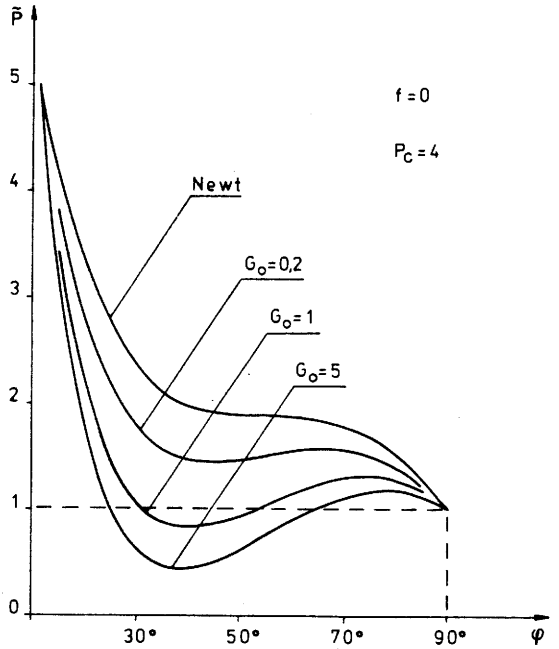

Fig. 12. Dimensionless pressure distributions for the flow between concentric spherical surfaces for $f = 0$ and $P_c = 4$.

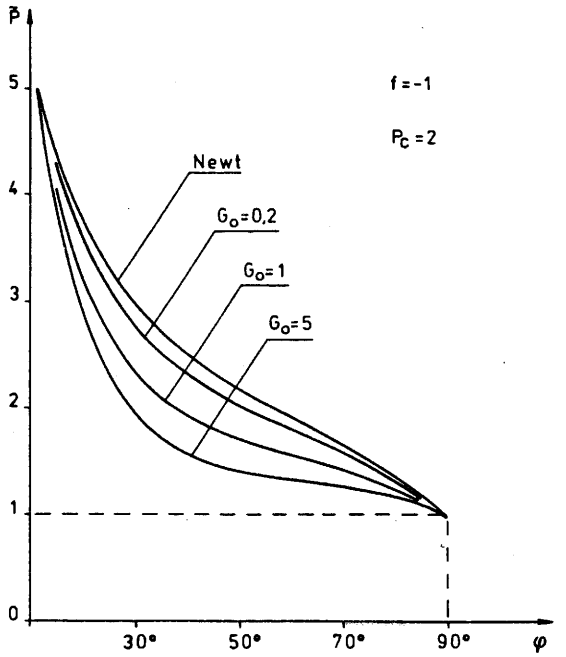

Fig. 13. Dimensionless pressure distributions for the flow between concentric spherical surfaces for $f = -1$ and $P_c = 2$.

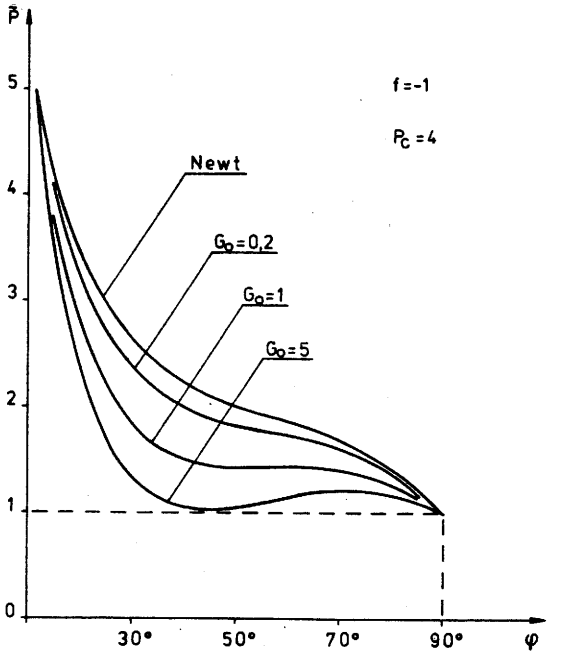

Fig. 14. Dimensionless pressure distributions for the flow between concentric spherical surfaces for $f = -1$ and $P_c = 4$.

The general nature of the graphs presented in these figures is similar to that for the flow between rotating disks, but in this case there is no flow with cavitation. Note that the character of changes of the velocity components $\widetilde{v}_x$ and $\widetilde{v}_\theta$ in this case of flow configuration is the same as in the previous one.

5. Conclusions

The analysis of the formulae derived allows us to confirm the fact that fluid flow in a slot is generated due to two reasons: the difference of pressures at the inlet and the outlet, and the rotational motion of the surfaces. It results from formula (25) that the profile of tangential velocity v_θ for the fixed cross – section is rectilinear and it is identical with the profile of Couette flow between two moving planes.

However, it results from the formulae for longitudinal velocity v_x that the main part — in approximation proposed here — has a profile identical with the profile of flat Poiseuille flow. This flow is generated by the difference of pressures and rotational motion of surfaces limiting the slot. The part of the secondary flow which is generated by the suction effect of the rotating surfaces is imposed on the main part of the longitudinal velocity.

The secondary flow is described by the second term of the formula for the longitudinal velocity v_x and by cross velocity v_y. From the formulae for pressure distributions it results that the inertia effect is considerable; it causes the pressure changes which increase with angular velocities of rotating surfaces. The influence of inertia forces is more visible in the flow between two disks (surfaces with rectilinear generatrices) than in that one between two spheres (surfaces with curvilinear generatrices). The nature of this influence depends on the magnitude of the plasticity coefficient G_0.

References

Buckhman Yu.B., Lipatov V.I., Litvinov A.I., Mitelman B.I. and Shulman Z.P. (1982): *Rheodynamics of non-linear viscoplastic media.* — J. Non-Newt. Fluid Mech., v.10, No.2, pp.215–233.

Coleman B.D., Markovitz H. and Noll W. (1966): *Viscometric Flows of Non-Newtonian Fluids.* — Berlin: Springer Verlag.

Dai G. and Bird R.B. (1981): *Radial flow of a Bingham fluid between two fixed circular disks.* — J. Non-Newt. Fluid Mech., v.8, No.3, pp.349–355.

Lipscomb C.C. and Dean M.M. (1984): *Flow of Bingham fluids in complex geometries.* — J. Non-Newt. Fluid Mech., v.14, No.3, pp.337–349.

McAlister K.W. and Rice W. (1970): *Throughflow between rotating surfaces of revolution, having similarity solution.* — Trans. ASME, J. Appl. Mech., ser. E, v.37, No.4, pp.924–930.

Prager W. (1961): *Introduction to Mechanics of Continua.* — Boston: Ginn.

Sandru N. and Camenschi G. (1988): *A mathematical model of the theory of tube drawing with floating plug.* — Int. J. Enging. Sci., v.26, No.6, pp.569–585.

Shulman Z.P. (1975): *Convective Heat Transfer of Rheologically Complex Fluids.* — Moscow: Energy (in Russian).

Walicka A. (1989): *Accurate and Asymptotic Solutions of Simplified Sets of Equations Describing the Motion of Viscous Fluids in a Slot Bounded by Two Co-Axial Surfaces of Revolution.* — Warszawa: WNT, (in Polish).

Walicka A. and Walicki E. (1994): *Viscoplastic flow between fixed surfaces of revolution. Analysis based on the averaged inertia.* — Report, Technical University of Zielona Góra, ser. Physics, No.6/7, pp.219–242. (in Polish).

Received: May 4, 1994
Revised: February 21, 1995